

Research Article

Analysis of the Immune and Antioxidant Response of Cellulose Nanocrystals Grafted with β -Cyclodextrin in Myeloid Cell Lines

Rajesh Sunasee , Melissa Carson, Hannah W. Despres, Angela Pacherille, Kaylee D. Nunez, and Karina Ckless 

Department of Chemistry, State University of New York at Plattsburgh, Plattsburgh, NY 12901, USA

Correspondence should be addressed to Rajesh Sunasee; rajesh.sunasee@plattsburgh.edu and Karina Ckless; kckle001@plattsburgh.edu

Received 1 August 2018; Revised 11 October 2018; Accepted 30 October 2018; Published 6 January 2019

Academic Editor: Ruibing Wang

Copyright © 2019 Rajesh Sunasee et al. This is an open access article distributed under the Creative Commons Attribution License, which permits unrestricted use, distribution, and reproduction in any medium, provided the original work is properly cited.

Cellulose nanocrystals (CNCs) have great potential in many areas of research, applications, and future commercialization prospects. Recently, CNCs have emerged as attractive candidates for biomedical applications such as drug and gene delivery systems. As such, cytotoxicity studies have been the major focus in the past decade. However, despite the rod-like nature of CNCs, the potential immune response of surface-modified CNCs is not well investigated. The current study examined the potential immune and antioxidant response induced by CNCs grafted with β -cyclodextrin (CNCs- β -CD) in a human monocyte cell line (THP-1) and a mouse macrophage-like cell line (J774A.1). We analyzed the secretion of the proinflammatory cytokine, interleukin 1 β (IL-1 β), by ELISA and mitochondria-derived reactive oxygen species (ROS) using fluorescence cell imaging and examined the intracellular levels of proteins involved in the immune and antioxidant response by immunoblotting. Our results indicated a dramatic increase neither in the IL-1 β secretion nor in the mitochondria-derived ROS resulting in no changes in the intracellular antioxidant response in THP-1 cells treated with different concentrations of CNCs- β -CD. Overall, CNCs- β -CD is nonimmunogenic and do not induce an increased antioxidant response under the conditions tested and hence has the potential to be used as a drug delivery carrier.

1. Introduction

During the past decades, the advancement in the discovery and design of new engineered nanomaterials for high-end sophisticated applications was on the rise and continues to have a huge impact on our everyday life [1–4]. Among those common nanomaterials such as carbon nanotubes, gold nanoparticles, quantum dots, and polymeric nanoparticles, nanocelluloses, in particular, cellulose nanofibrils (CNFs) and cellulose nanocrystals (CNCs), have emerged as a new class of natural and sustainable nanomaterials with exceptional physicochemical properties that have opened doors for a variety of potential applications [5–11]. CNCs, typically derived from acid hydrolysis of native cellulose, have recently surfaced as attractive candidates for biomedical applications due to their nanosized dimensions, biocompatibility, high specific surface area, high aspect ratio, and the presence of

numerous hydroxyl groups for chemical surface modifications [7, 9, 12–15].

Given the wide potential therapeutic applications of CNCs in addition to their needle-like morphological features, a thorough understanding of the interaction of CNCs with the biological system is crucial for investigating any possible associated health risks. From a toxicological point of view, several studies have shown that pristine CNCs, fluorescently labeled CNCs, and surface-modified CNCs exhibited low cytotoxicity under the conditions tested with various cell lines or aquatic species [16–22]. While cytotoxicity assessment is the first crucial step in determining the suitability of a material for biomedical applications, further detailed investigation of any potential immunological response is also recommended [12]. Nanoparticle immunogenicity has been under intense investigation in the past decades, and a significant progress has been achieved in understanding what

makes a nanomaterial immunogenic and the challenges it poses in the drug delivery field [23]. Some nanomaterials, especially those with cationic nature, have the ability to evoke an immune response. The immune response can be evaluated *in vitro* by secretion of proinflammatory cytokines, including interleukin 1 β (IL-1 β) [24]. The secretion of IL-1 β requires the synthesis of several intracellular proteins, including pro-IL-1 β and NOD-like receptor, pyrin domain containing 3 (NLRP3), known as “signal 1” or priming, followed by “signal 2” which is characterized by recruitment of the adaptor protein apoptosis-associated speck-like protein containing a CARD (ASC) and procaspase-1, leading to the processing and secretion of IL-1 β . It has been a consensus in the scientific literature that several identified NLRP3 activators also increase reactive oxygen species (ROS) [25] and, as a consequence, an antioxidant response is triggered by changing the levels of antioxidant enzymes [26]. Recently, we found that a CNCs cationic derivative (CNCs grafted with poly (N-(2-aminoethylmethacrylamide) (CNC-AEMA2)) evoked a robust inflammatory/immunological response in mouse and human macrophages, by inducing the secretion of the inflammatory cytokine interleukin-1 β (IL-1 β). This effect was associated with increases in mitochondrial ROS [27].

Cyclodextrins are cyclic oligosaccharides with a unique ability to form inclusion complexes with drug molecules, and as such, they have been commonly employed as materials in nanoparticle-based drug delivery systems [28]. The conjugation of CNCs with β -CD has been previously reported for drug delivery applications, but there are no studies on any potential immunological response of the surface-modified CNCs with β -CD [29, 30]. Herein, we reported, to the best of our knowledge, the first study that investigated the potential immune and antioxidant response induced by CNCs grafted with β -cyclodextrin in myeloid cells. Overall, this study will allow us to determine whether this nanoconjugate is immunogenic and hence its suitability for drug delivery applications.

2. Materials and Methods

2.1. Materials. Freeze-dried sulfated CNCs in their neutralized sodium salt forms were obtained from InnoTech Alberta located in Edmonton, Alberta, Canada. CNCs were prepared via traditional concentrated sulfuric acid hydrolysis of a Whatman™ cotton filter paper and are dispersible in water. β -Cyclodextrin, epichlorohydrin (99%), octylphenoxy polyethoxyethanol (Triton X-100), sodium dodecyl sulfate (SDS), β -mercaptoethanol (β -ME), and 4',6-diamidino-2-phenylindole (DAPI) were purchased from Sigma-Aldrich. UltraPure TEMED and mitochondrial superoxide indicator (MitoSOX™ Red) were obtained from Molecular Probes® (Invitrogen™). Lipopolysaccharide (LPS, *E. coli* 0111:B4) and phorbol myristate acetate (PMA) were purchased from InvivoGen. Antibodies against NLRP3 and IL-1 β were purchased from AdipoGen and BioVision, respectively. Antibodies against caspase-1, PrxSO₃, Prx1, and Trx2 were obtained from Abcam. SOD1 was purchased from Proteintech, and SOD2, Trx1, and β -actin (loading control) were purchased from Thermo Fisher. IgG horseradish peroxidase-

linked secondary mouse and rabbit antibodies were obtained from Abcam. Electrophoresis buffers and acrylamide solution were obtained from Bio-Rad Laboratories and iBlot® Transfer Stacks from Thermo Fisher. IL-1 β ELISA kits were purchased from BD Biosciences, and TMB ELISA substrate was purchased from R&D Systems. All reagents were of analytical grade.

2.2. Preparation of CNCs- β -CD. CNCs- β -CD was prepared according to a previously reported procedure with slight modifications [29]. β -CD (5.18 g, 4.56 mmol) was added to an aqueous NaOH solution (2 g NaOH dissolved in 10 mL of distilled water) followed by the addition of a homogenous suspension of CNCs (0.5 g in 10 mL of distilled water), and the mixture was stirred for 30 min. Epichlorohydrin (2.98 mL, 38 mmol) was then added into the reaction mixture, and the reaction was heated at 40°C for 6 h. The mixture was centrifuged at 12000 rpm for 30 min and washed repeatedly with distilled water to ensure the removal of both ungrafted β -CD and residual NaOH. The resulting product was resuspended in water and dialyzed against deionized water for 1 week with daily changes of water. The suspension was freeze-dried to afford a white flaky material (0.65 g).

2.3. Instrumentations

2.3.1. Fourier Transform Infrared Spectroscopy (FT-IR). FT-IR spectra of pristine and modified CNCs were recorded on a PerkinElmer FT-IR spectrophotometer (Spectrum Two) using freeze-dried samples at room temperature. KBr pellets were prepared by grinding in a mortar and compressing about 2% of the CNCs samples in KBr (previously well dried in an oven). Background measurement using neat KBr pellets was first acquired. Spectra in the range of 4000-400 cm⁻¹ were obtained with a resolution of 4 cm⁻¹ by cumulating 32 scans.

2.3.2. Zeta Potential and Dynamic Light Scattering (DLS) Measurements. Zeta (ζ) potential and DLS measurements were carried out using a Malvern Zetasizer Nano ZS instrument (model: ZEN3600; Malvern Instruments Inc., Westborough, MA, USA) at 25°C. This instrument is equipped with a 4.0 mW helium-neon laser ($\lambda = 633$ nm) and an avalanche photodiode detector and works at a 173° scattering angle. A 0.25 wt% CNCs dispersion in 10 mM NaCl was used for zeta potential while for DLS, the hydrodynamic apparent particle size was measured for 0.025 wt % CNCs dispersions in Milli-Q water. Both DLS and zeta potential measurements were performed at neutral pH. Results were recorded in triplicate, and the averages were reported.

2.4. Cell Culture and Experimental Conditions. The experimental conditions utilized in this manuscript are the same conditions utilized in the previously published manuscript [27]. Briefly, the mouse macrophage-like cell line J774A.1 and the human monocyte cell line THP-1 (both obtained from Sigma) were seeded at 3-5 \times 10⁵ cells/mL using RPMI 1640 medium (Gibco) supplemented with 10% fetal bovine serum (FBS), penicillin, streptomycin, and L-glutamine and incubated at 37°C in a 5% CO₂-supplemented atmosphere

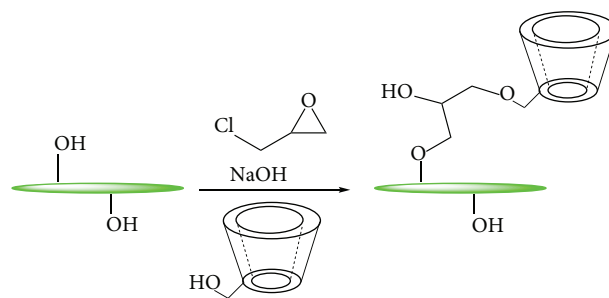
for at least 24 h before the appropriate treatments. THP-1 cells were stimulated with 3 ng/mL PMA, for 24 h prior to any treatment. J7744A.1 or PMA-stimulated THP-1 cells were primed with 100 ng/mL of LPS, and 4 h later, different concentrations of CNCs- β -CD were concomitantly added for a total of 24 h of total treatment.

2.5. SDS-PAGE and Immunoblotting. After respective treatments, total cell lysates were prepared by placing the tissue culture plates on ice. The attached cells were rinsed once with cold phosphate-buffered saline (PBS) and lysed using lysis buffer (50 mM Tris (pH 7.4), 150 mM NaCl, 2 mM EDTA, 0.2% Triton™ X-100, 0.3% IGEPAL®, and protease inhibitor cocktail). The lysates were scrapped from the plate and transferred to microcentrifuge tubes and immediately frozen in liquid nitrogen to prevent protein degradation and enhance cell lysis. Equal amounts of cell lysates were subjected to SDS-PAGE (12% sodium dodecyl sulfate polyacrylamide gels) and transferred from the gel to a polyvinylidene difluoride (PVDF) membrane. The membrane was blocked for 1 hour at room temperature with 5% milk in PBS containing 0.05% Tween®20 (PBST). After blocking, the membrane was rinsed with PBST and the primary antibodies were added and incubated on a rotating platform overnight at 4°C. The membrane was then rinsed three times for five minutes each with PBST, and the secondary antibodies were added with 5% milk and incubated on a rotating platform for 1 hour at room temperature. The membranes were developed using an enhanced chemiluminescence substrate (ECL, Pierce) according to the manufacturer's instructions, and membrane images captured using the ChemiDoc™ MP Imaging System coupled with Image Lab™ software.

2.6. Detection of IL-1 β in Cell Supernatants. IL-1 β secreted into the cell supernatants was quantified by enzyme-linked immunosorbent assay (ELISA) according to the manufacturer's instruction.

2.7. Detection of Mitochondria-Derived ROS. MitoSOX™ Red is a cell-permeable cationic dihydroethidium dye that is targeted to the mitochondria. Upon accumulation in the mitochondria, MitoSOX™ Red reacts with ROS to produce ethidium, which causes bright red fluorescence after binding to nucleic acids. In order to detect mitochondria-derived ROS, cells were loaded with 2.5 μ M MitoSOX™ Red. After 10 minutes at 37°C, the MitoSOX™ Red loading medium was removed, cells were rinsed with PBS, and nuclei were counterstained with DAPI for 5 min at room temperature. Live cell images were captured with a Bio-Rad ZOE™ Fluorescent Cell Imager, and the respective pictures were analyzed using ImageJ software.

2.8. Statistical Analysis. The data was statistically analyzed by using the one-way analysis of variance test, followed by Tukey's multiple comparison test, using GraphPad Prism 7.01 software. Statistical significance was defined as $P < 0.1$. All experiments were repeated at least twice, and for ELISA analysis, the experiments were also performed in triplicate.



SCHEME 1: Reaction scheme for the preparation of CNCs- β -CD.

3. Results and Discussion

3.1. Synthesis and Surface Analysis of CNCs- β -CD. Pristine CNCs, derived from sulfuric acid hydrolysis of a Whatman™ cotton filter paper, was reacted with β -CD and epichlorohydrin under a basic condition (Scheme 1). After the reaction, the product was isolated by several centrifugations and further purified by dialysis over a week to ensure the removal of unreacted materials and obtain a high-purity material. The resulting suspension was freeze-dried for two days to afford 0.65 g of a white flaky material. The overall grafting process was repeated three times with an average grafting efficiency of 15 wt% of β -CD covalently linked on the surface of CNCs which was obtained based on the previously reported method of weight measurement [29].

FT-IR spectroscopy was used to confirm the success of the reaction with a decrease in peak intensities located at 1161, 1113, and 1059 cm^{-1} and a peak broadening at 1033 cm^{-1} (C-O stretching band) for CNCs- β -CD when compared with pristine CNCs (Figure 1). The FT-IR results were in good agreement with previously reported values [29].

Next, the surface potential and colloidal stability of pristine CNCs and CNCs- β -CD were assessed by using zeta potential measurements, and in general, absolute zeta potential values above 20 mV are considered to be colloiddally stable [31]. Both pristine CNCs and CNCs- β -CD were found to be relatively stable colloids with a zeta potential values of -39.3 ± 0.7 mV and -24.1 ± 1.4 mV, respectively (Table 1). The negative zeta potential value of pristine CNCs is attributed to the presence of sulfate half-ester groups (OSO_3^-) arising during the sulfuric acid-mediated hydrolysis of cellulose. Furthermore, a decrease in the absolute zeta potential value from -39.3 ± 0.7 mV to -24.1 ± 1.4 mV is a good indication that modification of CNCs through the hydroxyl groups occurred, which eventually rendered the OSO_3^- less accessible. Dynamic light scattering (DLS) is a common tool used in the CNCs community for quickly measuring the relative particle size of CNCs as well as assessing the dispersion quality or aggregation state [32]. Fully dispersed CNCs- β -CD suspension (0.025 wt%) was analyzed by DLS, and an “apparent” particle size of 120.4 ± 4.3 nm was obtained (Table 1). An increase in the “apparent” particle size for CNCs- β -CD with respect to pristine CNCs (87.2 ± 1.5) could be attributed to the presence of grafted β -CD on the surface of CNCs.

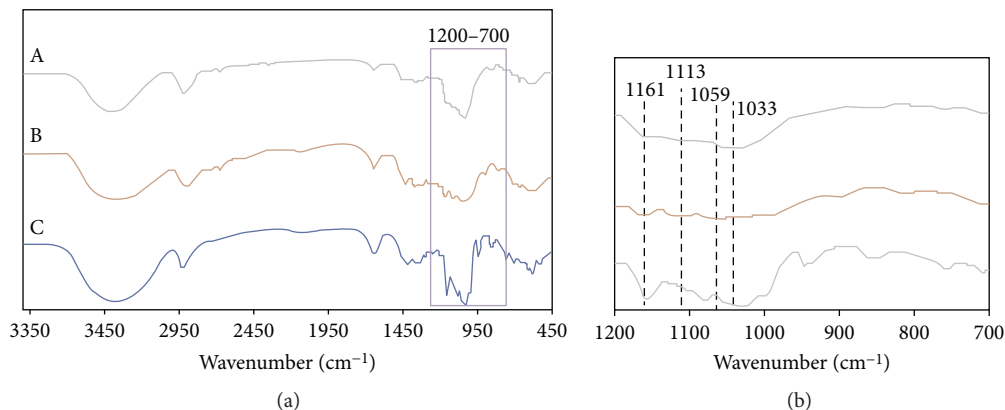


FIGURE 1: (a) FT-IR spectra of (A) CNCs- β -CD, (B) pristine CNCs, and (C) β -CD. (b) Expansion region of 1200-700 cm^{-1} showing pertinent peaks.

TABLE 1: DLS and zeta potential measurements of pristine CNCs and CNCs- β -CD.

Sample	Hydrodynamic "apparent" particle size (nm)	ζ -potentials (mV)
Pristine CNCs	87.2 ± 1.5	-39.3 ± 0.7
CNCs- β -CD	120.4 ± 4.3	-24.1 ± 1.4

3.2. CNCs- β -CD Does Not Induce a Strong Immunological Response in Human Monocytes. Nanoparticle surface coatings can impact both cytotoxicity and immunogenicity of nanosized biomedical materials [33]. We recently showed that CNCs- β -CD was not cytotoxic to mouse monocyte cells (J774A.1) and human breast adenocarcinoma cells (MCF-7) [21]. We now explore whether CNCs- β -CD can potentially evoke any inflammatory response in order to confirm its suitability as a nanodrug delivery vector. Activation of the NLRP3 inflammasome plays an important role in innate immunity, and the inflammatory response and the secretion of IL-1 β by immune cells can be indicative of this immunological response [34, 35]. Upon activation, the NLRP3 inflammasome is responsible for the activation of caspase-1, which in turn causes the release of cytokines such as IL-1 β . We have demonstrated that CNCs cationic derivatives with needle-like structure induced a strong immunological response in stimulated and nonstimulated human and mouse myeloid cells by activating NLRP3 inflammasome-dependent IL-1 β secretion [27]. Therefore, we sought to investigate whether a noncationic cellulose nanocrystal derivative, CNCs- β -CD, would also induce NLRP3 inflammasome activation and IL-1 β secretion in myeloid cells. Overall, the data indicated that CNCs- β -CD do not induce a strong immunological response in the human monocyte cell line (THP-1). In fact, a significant, but not dose-dependent, decrease in IL-1 β secretion by PMA-stimulated cells was observed. It was also observed that IL-1 β secretion is less in PMA-stimulated-only cells (controls, gray vs. black bars) than in LPS-treated cells, and the addition of CNCs- β -CD had a tendency to increase in a dose-dependent manner the IL-1 β secretion in PMA/LPS-stimulated cells, but this effect was not statistically significant (Figure 2(a)). We also

investigated the immune response of mouse macrophage-like cells (J774A.1) treated with CNCs- β -CD. The data indicated that CNCs- β -CD did not increase the secretion of IL-1 β (Figure 2(b)) or TNF α (Figure 2(c)) in this cell line, in any tested condition. It is important to mention that the lack of a significant immune response observed with CNCs- β -CD treatment in primed and nonprimed cells is not due to the intrinsic irresponsiveness of J774A.1 cells, since we have previously demonstrated that CNCs cationic derivatives (CNCs-AEMA2) induced a strong immunological response in this cell line in the absence of priming [27].

Since the IL-1 β secretion depends on the activation of the NLRP3 inflammasome including synthesis of its precursors (signal 1), next we analyzed the intracellular levels of NLRP3, procaspase-1, and pro-IL-1 β in PMA-stimulated THP-1 cells exposed to CNCs- β -CD, in the presence and absence of LPS. In general, major changes in the intracellular levels of NLRP3 and procaspase-1 were not observed in all conditions tested (Figure 3). However, there is a mild increase in pro-IL-1 β in LPS-stimulated cells upon CNCs- β -CD treatment as the bands darken with increasing concentrations of nanomaterials (Figure 3). This event is consistent with the tendency to increase IL-1 β secretion in the same experimental conditions (Figure 2). The potential immunostimulatory effect of CNCs- β -CD in the presence of LPS is not surprising, since it has been reported that some needle-like nanomaterials can activate the NLRP3 inflammasome/IL-1 β axis [27, 36] mainly in the presence of LPS.

3.3. CNCs- β -CD Alone Enhances Mitochondrial ROS Production, but It Does Not Affect the Antioxidant Defenses.

The mitochondria are responsible for many of the metabolic processes that occur within the cell. Under normal resting conditions, the mitochondria produce a certain amount of ROS as a by-product of the electron transport chain, which can increase in more active mitochondria. However, upon stress conditions, including inflammation, the mitochondria can produce even greater amounts of ROS [37–39]. In fact, we have demonstrated that substantial increases in mitochondria-derived ROS are associated with NLRP3 inflammasome activation [27, 40]. Using MitoSOX, a probe that specifically targets the mitochondria, changes in ROS

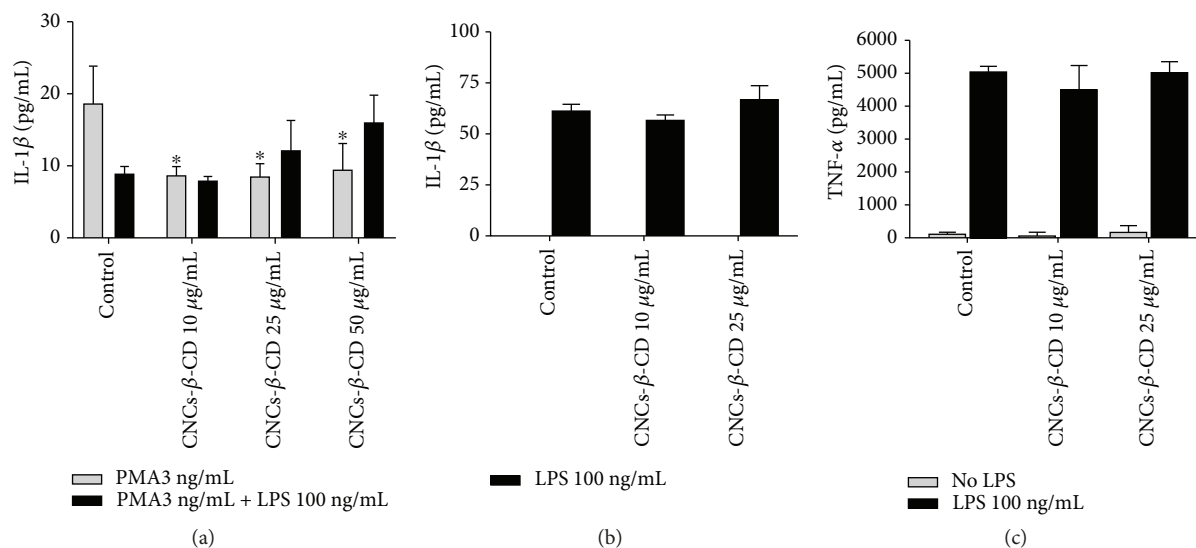


FIGURE 2: Immunological response of human and mouse cells treated with cellulose nanocrystal- β -cyclodextrin (CNCs- β -CD), in the presence or absence of lipopolysaccharide (LPS, 100 ng/mL). THP-1 cell lines were initially incubated with phorbol 12-myristate 13-acetate (PMA, 3 ng/mL) for 24 h and then concomitant with LPS (100 ng/mL) for 4–5 h followed by the addition of CNCs- β -CD (10–50 μ g/mL) for another 19–20 h. Secreted (a) IL-1 β by THP-1 was quantified in the cell supernatants by ELISA. Alternatively, mouse macrophage-like cells (J774A.1) were treated with LPS (100 ng/mL) for 4–5 h followed by the addition of CNCs- β -CD (25 and 50 μ g/mL) for another 19–20 h. Secreted (b) IL-1 β and (c) TNF α by J774A.1 were quantified in the cell supernatants by ELISA. Data were means \pm SD from triplicate. * $P < 0.1$ compared to respective control.

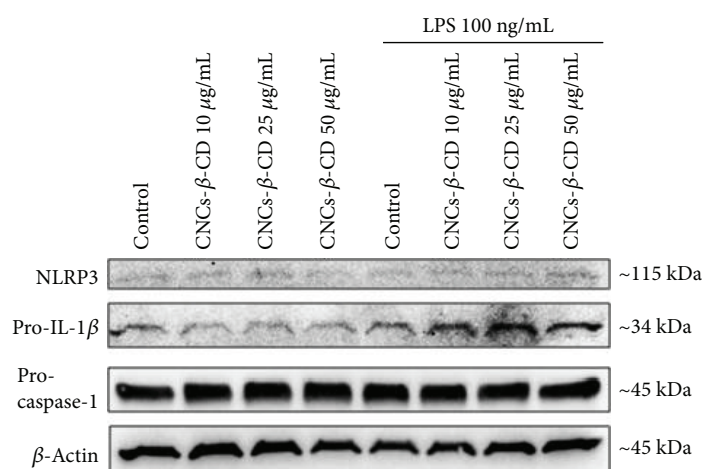


FIGURE 3: Immunological response of PMA-stimulated THP-1 cells of CNCs- β -CD, in the presence or absence of lipopolysaccharide (LPS, 100 ng/mL). THP-1 cell lines were treated as in Figure 2, and the intracellular inflammasome components (NLRP3, procaspase-1, and pro-IL-1 β) were analyzed by western blotting in the cell lysates. β -Actin was used as a loading control.

production can be visualized since red fluorescent color intensity increases as the amounts of ROS also increases. Overall, in the mouse macrophage-like cell line, the highest concentration of CNCs- β -CD alone caused an increase in mitochondrial ROS production (Figure 4). However, when combined with LPS, CNCs- β -CD appeared to have a protective effect against mitochondrial ROS production. As expected, the control cells that only received LPS displayed greater ROS production than all the cells treated with LPS and CNCs- β -CD (Figure 4, gray bar, second set on the graph).

Antioxidant enzymes are released in response to an increase in intracellular ROS production. These proteins are responsible for the degradation of ROS in order to prevent cell toxicity [41, 42]. Next, we investigated whether the increases in mitochondria-derived ROS could impact the antioxidant defenses, by changing the intracellular levels of the major antioxidant enzymes. Overall, results indicated that in the PMA-stimulated human monocyte-like cells (THP-1), CNCs- β -CD in the presence or absence of LPS did not cause significant changes in the level of the majority of antioxidant enzymes, using western blotting analysis

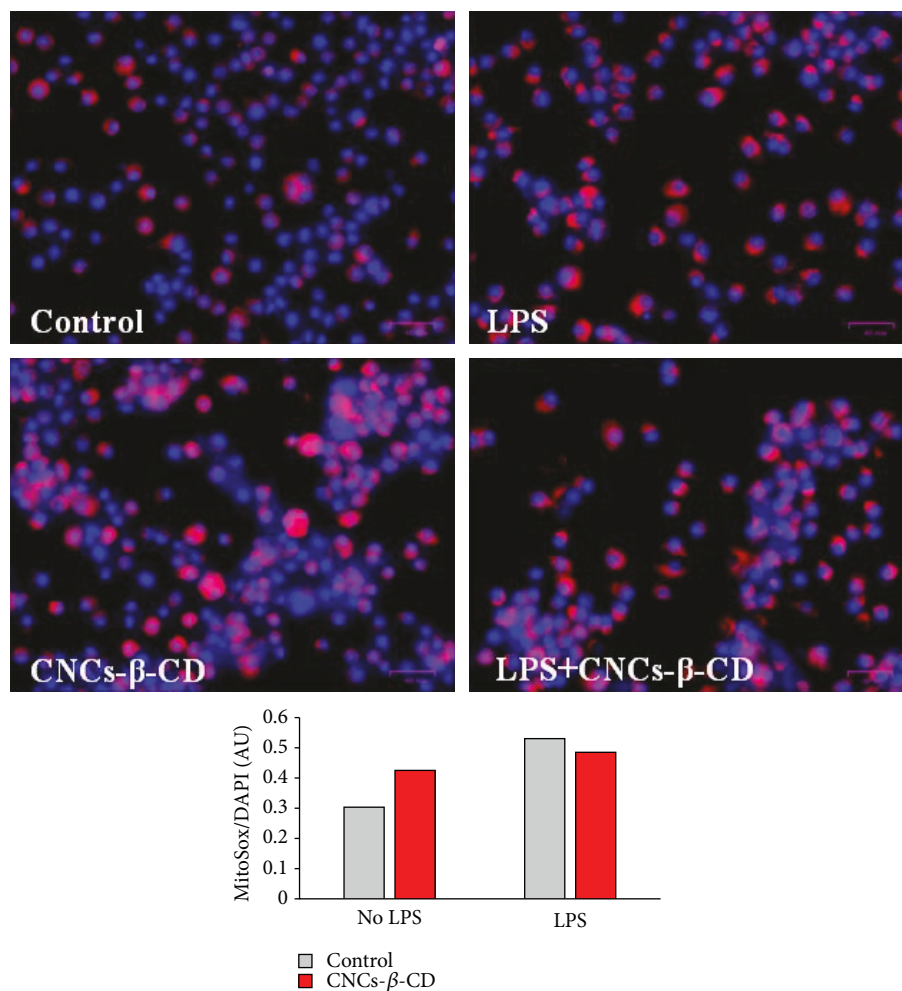


FIGURE 4: Effect of CNCs- β -CD on the changes in mitochondrial ROS in LPS-primed macrophages. Mouse macrophage-like cells (J774A.1) were stimulated with LPS (100 ng/mL) for 4-5 h followed by concomitant treatment with CNCs- β -CD (50 μ g/mL) for another 19-20 h. After treatment, MitoSOX Red was added to the live cells for 10 min, followed by DAPI (1 μ g/mL) for an additional 5 min. Mitochondrial ROS levels were promptly analyzed utilizing the ZOE™ Fluorescent Cell Imager (scale bar = 40 μ m). The pixel intensity was analyzed using ImageJ and expressed as integrated intensity (graph on the bottom of the figure).

(Figure 5). The only antioxidant enzyme that appeared to have an augmented intracellular level was oxidized peroxiredoxins (PrxSO₃). The mechanism by which these enzymes exert their function as an antioxidant is becoming oxidized per se indicated by the oxidation of specific thiol groups in their active sites, forming -SO₃⁻, which can be detected by western blotting. Therefore, this mild increase in the presence of LPS is not totally unexpected because the peroxiredoxins are ubiquitous antioxidant enzymes which are the primary defense mechanisms against ROS, even in low amounts [43]. When the peroxiredoxins fulfill their function as a primary antioxidant defense, it is reasonable to assume that no further increases in other antioxidant enzymes are necessary. To investigate further this potentially oxidative event, we also analyzed hyperoxidation and consequent aggregation of peroxiredoxin 1 (Prx1). Upon highly oxidizing conditions, such as in the presence of high levels of H₂O₂, hyperoxidized peroxiredoxins in some species can form high molecular weight multimers [43]. The data

revealed no changes on the levels of Prx1 or formation of high molecular weight complexes (Figure 5). This data indicates that the potential oxidative event observed with mild increases in PrxSO₃ is not sufficient to cause hyperoxidation of Prx1.

4. Conclusions

In conclusion, although not statistically significant, CNCs- β -CD showed a tendency to increase IL-1 β secretion in LPS-stimulated human cells at higher concentrations. We did not observe dramatic increases in the intracellular inflammatory responses induced by CNCs- β -CD in comparison with other CNCs derivatives previously studied [27]. We also did not observe any dramatic changes in the intracellular antioxidant response in cells treated with different concentrations of CNCs- β -CD. The mild impact on redox balance coincides with the lack of significant immunogenicity observed with CNCs- β -CD treatments in PMA-stimulated

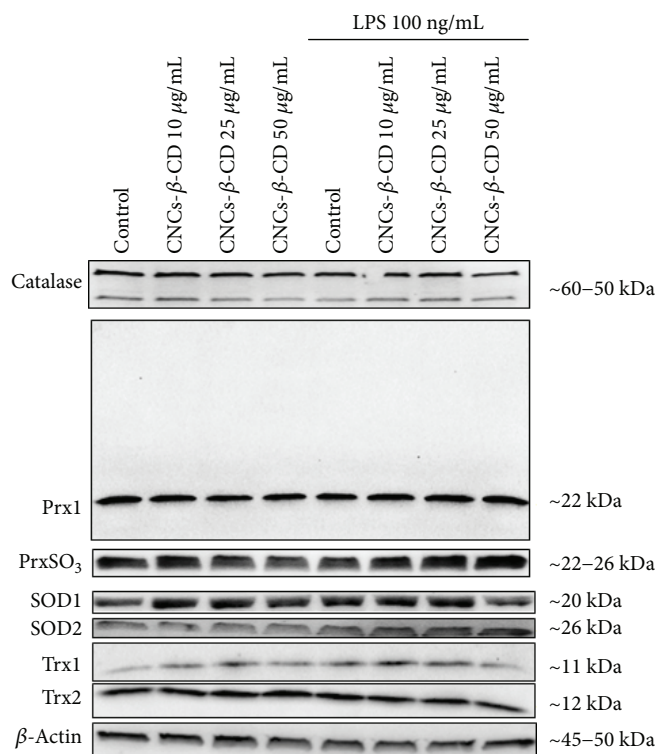


FIGURE 5: Antioxidant response of PMA-stimulated THP-1 cells of cellulose nanocrystal- β -cyclodextrin (CNC- β -CD), in the presence or absence of lipopolysaccharide (LPS, 100 ng/mL). THP-1 cell lines were treated as in Figure 2, and the intracellular antioxidant enzymes, including catalase, peroxiredoxin 1 (Prx1), oxidized peroxiredoxins (PrxSO₃), superoxide dismutases 1 and 2 (SOD1 and mitochondrial SOD2), and thioredoxins 1 and 2 (Trx1 and mitochondrial Trx2), were analyzed by western blotting in the cell lysates. β -Actin was used as a loading control.

human monocytes. Overall, our results indicated that CNCs- β -CD is nonimmunogenic and does not induce major oxidative stress in the conditions tested, suggesting that it can be used in biomedical applications such as drug delivery systems. However, further comprehensive *in vitro* and *in vivo* testing must be performed to confirm its safety and effectiveness.

Data Availability

The data used to support the findings of this study are included within the article. Any more specific details in the data will be delivered by the corresponding authors upon request.

Conflicts of Interest

The authors declare that there is no conflict of interest regarding the publication of this paper.

Acknowledgments

This material is based upon the work supported by the National Science Foundation under Grant no. 1703890. This work was also partly supported by the State University of New York Plattsburgh Presidential Research Award 2017-2018.

References

- [1] R. Petros and J. M. DeSimone, "Strategies in the design of nanoparticles for therapeutic applications," *Nature Reviews Drug Discovery*, vol. 9, no. 8, pp. 615–627, 2010.
- [2] J. Jeevanandam, A. Barhoum, Y. S. Chan, A. Dufresne, and M. K. Danquah, "Review on nanoparticles and nanostructured materials: history, sources, toxicity and regulations," *Beilstein Journal of Nanotechnology*, vol. 9, pp. 1050–1074, 2018.
- [3] C. Sun, H. Zhang, S. Li et al., "Polymeric nanomedicine with "Lego" surface allowing modular functionalization and drug encapsulation," *ACS Applied Materials & Interfaces*, vol. 10, no. 30, pp. 25090–25098, 2018.
- [4] G. Gao, F. Tang, G. Gong et al., "pH-responsive prodrug nanoparticles based on a sodium alginate derivative for selective co-release of doxorubicin and curcumin into tumor cells," *Nanoscale*, vol. 9, no. 34, pp. 12533–12542, 2017.
- [5] D. Klemm, F. Kramer, S. Moritz et al., "Nanocelluloses: a new family of nature-based materials," *Angewandte Chemie International Edition*, vol. 50, no. 24, pp. 5438–5466, 2011.
- [6] R. J. Moon, A. Martini, J. Nairn, J. Simonsen, and J. Youngblood, "Cellulose nanomaterials review: structure, properties and nanocomposites," *Chemical Society Reviews*, vol. 40, no. 7, pp. 3941–3994, 2011.
- [7] N. Lin and A. Dufresne, "Nanocellulose in biomedicine: current status and future prospect," *European Polymer Journal*, vol. 59, pp. 302–325, 2014.

- [8] Y. Habibi, "Key advances in the chemical modification of nanocelluloses," *Chemical Society Reviews*, vol. 43, no. 5, pp. 1519–1542, 2014.
- [9] M. Jorfi and E. J. Foster, "Recent advances in nanocellulose for biomedical applications," *Journal of Applied Polymer Science*, vol. 132, no. 14, pp. 41719–41737, 2015.
- [10] M. Kaushik and A. Moores, "Review: nanocelluloses as versatile supports for metal nanoparticles and their applications in catalysis," *Green Chemistry*, vol. 18, no. 3, pp. 622–637, 2016.
- [11] K. J. De France, T. Hoare, and E. D. Cranston, "Review of hydrogels and aerogels containing nanocellulose," *Chemistry of Materials*, vol. 29, no. 11, pp. 4609–4631, 2017.
- [12] R. Sunasee, U. D. Hemraz, and K. Ckless, "Cellulose nanocrystals: a versatile nanoplatform for emerging biomedical applications," *Expert Opinion on Drug Delivery*, vol. 13, no. 9, pp. 1243–1256, 2016.
- [13] S. Eyley and W. Thielemans, "Surface modification of cellulose nanocrystals," *Nanoscale*, vol. 6, no. 14, pp. 7764–7779, 2014.
- [14] J. K. Jackson, K. Letchford, B. Z. Wasserman, L. Ye, W. Y. Hamad, and H. M. Burt, "The use of nanocrystalline cellulose for the binding and controlled release of drugs," *International Journal of Nanomedicine*, vol. 6, pp. 321–330, 2011.
- [15] A. B. Seabra, J. S. Bernardes, W. J. Fávaro, A. J. Paula, and N. Durán, "Cellulose nanocrystals as carriers in medicine and their toxicities: a review," *Carbohydrate Polymers*, vol. 181, pp. 514–527, 2018.
- [16] T. Kovacs, V. Naish, B. O'Connor et al., "An ecotoxicological characterization of nanocrystalline cellulose (NCC)," *Nanotoxicology*, vol. 4, no. 3, pp. 255–270, 2010.
- [17] S. Dong, A. A. Hirani, K. R. Colacino, Y. W. Lee, and M. Roman, "Cytotoxicity and cellular uptake of cellulose nanocrystals," *Nano LIFE*, vol. 2, no. 3, article 1241006, 2012.
- [18] K. A. Mahmoud, J. A. Mena, K. B. Male, S. Hrapovic, A. Kamen, and J. H. T. Luong, "Effect of surface charge on the cellular uptake and cytotoxicity of fluorescent labeled cellulose nanocrystals," *ACS Applied Materials Interfaces*, vol. 2, no. 10, pp. 2924–2932, 2010.
- [19] K. B. Male, A. C. W. Leung, J. Montes, A. Kamen, and J. H. T. Luong, "Probing inhibitory effects of nanocrystalline cellulose: inhibition versus surface charge," *Nanoscale*, vol. 4, no. 4, pp. 1373–1379, 2012.
- [20] U. D. Hemraz, K. A. Campbell, J. S. Burdick, K. Ckless, Y. Boluk, and R. Sunasee, "Cationic poly(2-aminoethylmethacrylate) and poly(*N*-2-aminoethylmethacrylamide) modified cellulose nanocrystals: synthesis, characterization, and cytotoxicity," *Biomacromolecules*, vol. 16, no. 1, pp. 319–325, 2015.
- [21] A. S. Jimenez, F. Jaramillo, U. D. Hemraz, Y. Boluk, K. Ckless, and R. Sunasee, "Effect of surface organic coatings of cellulose nanocrystals on the viability of mammalian cell lines," *Nanotechnology, Science and Applications*, vol. 10, pp. 123–136, 2017.
- [22] M. Roman, "Toxicity of cellulose nanocrystals: a review," *Industrial Biotechnology*, vol. 11, no. 1, pp. 25–33, 2015.
- [23] A. N. Ilinskaya and M. A. Dobrovolskaia, "Understanding the immunogenicity and antigenicity of nanomaterials: past, present and future," *Toxicology and Applied Pharmacology*, vol. 299, pp. 70–77, 2016.
- [24] M. Zaitseva, T. Romantseva, K. Blinova et al., "Use of human MonoMac6 cells for development of in vitro assay predictive of adjuvant safety in vivo," *Vaccine*, vol. 30, no. 32, pp. 4859–4865, 2012.
- [25] F. Martinon, "Signaling by ROS drives inflammasome activation," *European Journal of Immunology*, vol. 40, no. 3, pp. 616–619, 2010.
- [26] P. Moller, D. V. Christophersen, D. M. Jensen et al., "Role of oxidative stress in carbon nanotube-generated health effects," *Archives of Toxicology*, vol. 88, no. 11, pp. 1939–1964, 2014.
- [27] R. Sunasee, E. Araoye, D. Pyram, U. D. Hemraz, Y. Boluk, and K. Ckless, "Cellulose nanocrystal cationic derivative induces NLRP3 inflammasome-dependent IL-1 β secretion associated with mitochondrial ROS production," *Biochemistry and Biophysics Reports*, vol. 4, pp. 1–9, 2015.
- [28] H. Shelley and J. Babu, "Role of cyclodextrins in nanoparticle-based drug delivery systems," *Journal of Pharmaceutical Sciences*, vol. 107, no. 7, pp. 1741–1753, 2018.
- [29] N. Lin and A. Dufresne, "Supramolecular hydrogels from in situ host-guest inclusion between chemically modified cellulose nanocrystals and cyclodextrin," *Biomacromolecules*, vol. 14, no. 3, pp. 871–880, 2013.
- [30] G. M. A. N. Ntoutoume, R. Granet, J. P. Mbakidi et al., "Development of curcumin–cyclodextrin/cellulose nanocrystals complexes: new anticancer drug delivery systems," *Bioorganic & Medicinal Chemistry Letters*, vol. 26, no. 3, pp. 941–945, 2016.
- [31] S. Bhattacharjee, "DLS and zeta potential-what they are and what they are not?," *Journal of Controlled Release*, vol. 235, pp. 337–351, 2016.
- [32] E. J. Foster, R. J. Moon, U. P. Agarwal et al., "Current characterization methods for cellulose nanomaterials," *Chemical Society Reviews*, vol. 47, no. 8, pp. 2609–2679, 2018.
- [33] O. Gamucci, A. Bertero, M. Gagliardi, and G. Bardi, "Biomedical nanoparticles: overview of their surface immune-compatibility," *Coatings*, vol. 4, no. 1, pp. 139–159, 2014.
- [34] B. Z. Shao, Z. Q. Xu, B. Z. Han, D. F. Su, and C. Liu, "NLRP3 inflammasome and its inhibitors: a review," *Frontiers in Pharmacology*, vol. 6, p. 262, 2015.
- [35] S. M. Man and T. D. Kanneganti, "Converging roles of caspases in inflammasome activation, cell death and innate immunity," *Nature Reviews Immunology*, vol. 16, no. 1, pp. 7–21, 2016.
- [36] J. Palomaki, E. Valimaki, J. Sund et al., "Long, needle-like carbon nanotubes and asbestos activate the NLRP3 inflammasome through a similar mechanism," *ACS Nano*, vol. 5, no. 9, pp. 6861–6870, 2011.
- [37] K. E. Lawlor and J. E. Vince, "Ambiguities in NLRP3 inflammasome regulation: is there a role for mitochondria?," *Biochimica et Biophysica Acta (BBA) - General Subjects*, vol. 1840, no. 4, pp. 1433–1440, 2014.
- [38] R. Zhou, A. S. Yazdi, P. Menu, and J. Tschopp, "A role for mitochondria in NLRP3 inflammasome activation," *Nature*, vol. 469, no. 7329, pp. 221–225, 2011.
- [39] J. Tschopp, "Mitochondria: sovereign of inflammation?," *European Journal of Immunology*, vol. 41, no. 5, pp. 1196–1202, 2011.
- [40] J. Jabaut, J. L. Ather, A. Taracanova, M. E. Poynter, and K. Ckless, "Mitochondria-targeted drugs enhance Nlrp3 inflammasome-dependent IL-1 β secretion in association with alterations in cellular redox and energy status," *Free Radical Biology and Medicine*, vol. 60, pp. 233–245, 2013.
- [41] H. Y. Yang and T. H. Lee, "Antioxidant enzymes as redox-based biomarkers: a brief review," *BMB Reports*, vol. 48, no. 4, pp. 200–208, 2015.

- [42] E. Birben, U. M. Sahiner, C. Sackesen, S. Erzurum, and O. Kalayci, "Oxidative stress and antioxidant defense," *World Allergy Organizational Journal*, vol. 5, no. 1, pp. 9–19, 2012.
- [43] S. G. Rhee, "Overview on peroxiredoxin," *Molecules and Cells*, vol. 39, no. 1, pp. 1–5, 2016.

